Detection Method of Scallop and Asteroid from Seabed Video

Koichiro ENOMOTO
Future University Hakodate, Japan
116-2 Kamedanakano-cho, Hakodate,
Hokkaido, Japan
e-mail g3111001@fun.ac.jp

Masashi TODA
Kumamoto University, Japan
2-39-1, Kurokami, Kumamoto, Japan
e-mail toda@cc.kumamoto-u.ac.jp

Yasuhiro KUWAHARA
Hokkaido Abashiri Fisheries
Experiment Station, Japan
1-1-1 Masuura, Abashiri,
Hokkaido Japan

Abstract

Recently, the investigation method has been developed to measure fishes using an underwater video camera. These methods can investigate the benthic fishery resources, but the acoustic survey cannot. However, these investigations do not use automatic measurements from the videos but only taken the videos. In this paper, we propose a method to count the scallop and the asteroid from the seabed videos, present the results, and evaluate the method's effectiveness. We also show the fishery resource maps of the scallop and the asteroid using the GPS data.

1 Introductions

Recently, the investigation method has been developed to measure fishes using an underwater camera or an underwater video camera [1, 2]. These methods can investigate the benthic fishery resources, but the acoustic survey cannot. However, these investigations do not use automatic measurements from the images and the videos but only taken images [1, 2].

In the scallop culture industry in Abashiri, Japan, the fisheries are investigated by analyzing seabed images [1]. The results of investigations are used to estimate the catch size, time fish are caught, and future stocks. K. Enomoto et al. showd a method to extract the scallop area from the seabed images in the fields of gravel [3] and sand [4]. However, this investigation need to apply the seabed videos, because of the investigations must more accurately measure the numbers, sizes, and states of fisheries.

In this paper, we propose a method to count the scallop and the asteroid from the seabed videos, present the results, and evaluate the method's effectiveness. We also show the fishery resource maps of the scallop and the asteroid using the GPS data.

2 Design Consideration

2.1 Seabed Video

Figure 1 shows the simplified schematic of the shooting equipment for the seabed video. The shooting equipment is a metallic frame, a digital video camera, a lighting. The legs of equipment are a sled-like structure. The shooting equipment glide over the seabed. Therefore, the height of the video camera is stabilized.

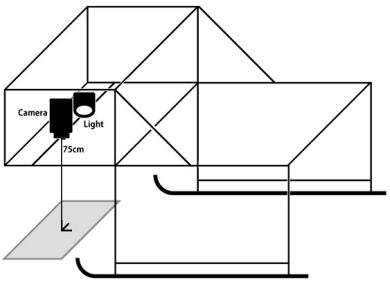

Figure 1. Simplified schematic of the shooting equipment for the seabed video.

Figure 2. Sample of the seabed video.

Figure 2 shows a sample frame of the seabed video. The video size is 1920×1024, frame rate is 30fps, and it is in 24-bit color. The object sea region is Notsuke, Japan, the bottom sediment is sand. The videos include scallop, asteroid, debris of scallop shell.

The fishery investigation also record GPS data while the recording of the seabed videos. Therefore, we can know the position of the seabed videos for GPS data.

2.2 Scallop and Asteroid

Figure 3 shows the scallop regions and the asteroid regions in the seabed video.

In Fig. 3(a) and (b), the scallop regions have special features such as the shelly rims being white and shaped like fans. On the scallop shell, the black regions are algae. The scallop opens and closes its shell while it is alive and breathing. For the same reason, the scallop does not overlap with other scallops. This is based on

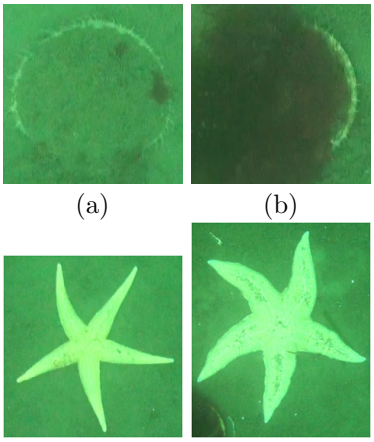

(a) (b) (c) (d)

Figure 3. The images of the scallop and the asteroid. The scallop region images are (a) and (b). The asteroid region images are (c) and (d).

the professional knowledge of ecologists and fisherman.

In this paper, we target the asteroid *Asterias amurensis* of white, because this asteroid has considerable individual variability such as color and pattern. In Fig. 3(c) and (d), the asteroid regions have being white, the legs are five, and the various sizes.

3 Proposed Method

3.1 Proposed Method

Our proposed method to count the scallop and the asteroid are described below. First, the asteroids are detected from the seabed video, because the algorithm to detect the scallop detect incorrectly the asteroid [4]. Next, the scallops are detected from the seabed video.

3.2 Detection Method of Asteroid

Our proposed method to detect the asteroid is described below.

1. Binarization
2. Detect the asteroid using the shape feature.

First, the white regions are extracted from the seabed videos. Next, the process removes the noise from the extracted regions. Finally, the asteroids are detected using the shape feature.

3.2.1 Extract the Asteroid Regions

In general, the asteroid's body is white or yellow. We define the color feature as the whiteness of the asteroid. The asteroid is defined as a lightness that has a high value in the local regions. However, it is difficult to extract the asteroid regions using static threshold processing. We describe the method to extract the asteroid regions using dynamic threshold [4].

An image I, a region R of the size (W, H) in the image I, the mean of lightness L_μ in a region R, and the standard deviation σ are denoted. When a threshold $Th_c(x, y)$ of an image $I(x, y)$ is defined as

$$Th_c(x, y) = L_\mu + \lambda L_\sigma, \tag{1}$$

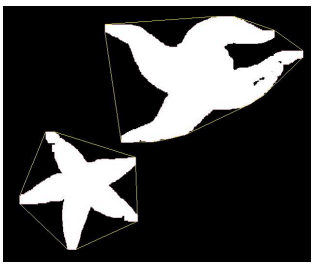

Figure 4. Result of binalization. The yellow lines are the convex hull lines of the object region. The object image is the crip region of Fig. 2

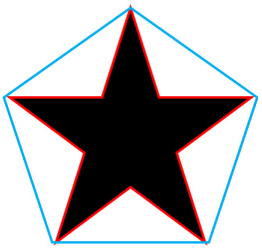

Figure 5. The object region (Red) and the convex hull region (Blue).

where, λ is set by the rate of a confidence interval of background when the histogram of a region R is assumed to have normal distribution. Here, if the threshold Th_c is higher than Th_{upper}, we define it as $Th_c = Th_{upper}$, because the lightness value is limited.

In this paper, a region R is the local region of the size $(W, H) = 64$ and all image of the size $(W, H) = (1920, 1080)$, because the asteroid have considerable individual variability of color and the seabed images differ in the illumination.

The extracted regions include the noise such as the debris of the shell and the san. Therefore, in post-processing, the extracted regions are removed to be dilation, erosion, and the threshold processing to areas. The result image of the threshold processing is shown Fig. 4.

3.2.2 Detect Asteroid

The positions of the asteroid's legs differ vastly (Fig. 2). In this paper, the asteroid is detected using the shape of the asteroid.

An area S of the extracted region and an area S_C of the convex hull region of the extracted region are denoted (Fig. 5). When, the ratio ρ of the area S to S_C is defined as

$$\rho = \frac{S}{S_C} \qquad (0 \leq \rho \leq 1). \tag{2}$$

The asteroid region is detected, when the rate ρ satisfies

$$\rho \leq Th_\rho, \tag{3}$$

where Th_ρ is threshold of the rate ρ. In this paper, we set the threshold $Th_\rho = 0.75$.

3.3 Detection Method of Scallop

The method to detect the scallop is described below [4].

1. Extract the candidate pixels of the scallop's shelly rim
2. Extract the candidate regions of the scallop
3. Detect the scallop

The candidate shelly rim pixels are extracted from the seabed video by dynamic threshold processing. Next, the candidate scallop regions are extracted using the Hough transform to extract the ellipse. Finally, the scallop regions are extracted by threshold processing using the shelly rim feature and the shell feature.

3.3.1 Candidate of Shelly Rim

In the sand fields, there is no sand in the shelly rim, but the scallop shell is covered with sand because the scallop opens and closes its shell while it is alive and breathing (Fig. 3(a), (b)). In general, the scallop's shelly rim is white. The color feature of the scallop's shelly rim is defined as the whiteness.

The candidate pixels of the scallop's shelly rim are extracted using the dynamic threshold processing of Sec. 3.2.1. In this paper, we use the threshold processing to the local region and set $(W, H) = (64, 64)$.

3.3.2 Extract the Candidate Scallops

The scallop's shell is shaped like a fan. The shape of the scallop shell is defined as an ellipse and extracts it using the Hough transform to detect ellipses. An ellipse is defined as $f(x, y, \alpha, \beta, \phi)$ by five parameters: the center point (x_0, y_0), two semi-axes (α and β), and an orientation ϕ. These parameters are determined by voting in the Hough parameter space. Here, a parameter of the orientation is set at $\phi = 0$, because, the shape of a shelly rim is less than half an ellipse (Fig. 3(a), (b)). Therefore, the Hough transform uses the four-dimensional parameter space. The extracted ellipses are the candidates for the scallop regions.

The feature points are the candidate pixels of the scallop's shelly rim. Since the scallop regions have sizes in a constant range that is known in the seabed video. We can set two semi-axes at $120 \leq \alpha, \beta \leq 200$.

3.3.3 Detect of Scallop

The scallop's shell is a fan-like shape and the shelly rim is white. Therefore, if these pixels are the scallop's shelly rim, the candidate pixels of the shelly rim follow the scallop's rim.

In Hough transform, $\Delta\alpha$ and $\Delta\beta$ denote the resolutions of parameter space. When Q denote the near region of this elliptic boundary $f(x, y, \alpha, \beta)$ has the feature points that were voted. A region Q is

$$f(x, y, \alpha - \frac{\Delta\alpha}{2}, \beta - \frac{\Delta\beta}{2}) \leq Q \leq f(x, y, \alpha + \frac{\Delta\alpha}{2}, \beta + \frac{\Delta\beta}{2}). \quad (4)$$

A vote number of the parameter space is the same as number of the feature points on a region Q.

The boundary length of the ellipse l and the parameter $\frac{1}{D}(0 < \frac{1}{D} \leq 1)$ are defined. In the range of $\frac{1}{D}l$, the maximum number of the feature points on a region Q is calculated, and denoted as Num_Q. Here, the value of the shelly rim feature R_Q is defined as

$$R_Q = \frac{Num_Q}{\frac{1}{D}l}. \quad (5)$$

Table 1. Experiment results of the scallop.

Detection Num.(tp)	70
Non-Detection Num.(tn)	16
Error Detection Num.(fn)	20
Detection Rate	81.40%
Error Rate	22.22%

In the candidate area, the region of an inside region Q denoted as $\bar{Q}$. The number of the candidate pixels on $\bar{Q}$ is calculated, and denoted as $Num_{\bar{Q}}$. Here, the rate of its $R_{\bar{Q}}$ is defined as

$$R_{\bar{Q}} = \frac{Num_{\bar{Q}}}{\bar{Q}}. \quad (6)$$

We defined the scallop region when R_Q and $R_{\bar{Q}}$ satisfy

$$Th_Q \leq R_Q \cap R_{\bar{Q}} \leq Th_{\bar{Q}} \quad (7)$$

where Th_Q is the threshold for the shelly rim feature R_Q and $Th_{\bar{Q}}$ is the threshold for the inside a shelly rim feature $R_{\bar{Q}}$.

4 Experiment

4.1 Method

In this experiment, we used 12 minutes and 10 seconds seabed video that contained 86 scallops and 293 asteroids. The evaluation methods are devined as below. In all detected region, if an object region was detected correctly, we determined the results to be true-positive tp. If an object region was not detected, we determined the results to be true-negative tn. Furthermore, if non-object region was detected, we determined the results to be false-negative fn. A detection rate and an error rate are defined as

$$Detectionrate = \frac{tp}{tp + tn} 100[\%], \quad (8)$$

$$Errorrate = \frac{fn}{tp + fn} 100[\%]. \quad (9)$$

4.2 Results

The sample of the experiment result is shown in Fig. 6. In Fig. 6, 1 scallop and 2 asteroids are existed and were detected correctly.

The results of the experiment to detect the scallop are shown in Table 1, the results of the experiment to detect the asteroid are shown in Table 2. The extraction rate accuracy of the scallop region is 81.40% and the error rate accuracy is 22.22%. In the error cases, the many regions were detected in the ballas field (like the debris of shell).

The extraction rate accuracy of the asteroid region is 99.66% and the error rate accuracy is 0.68%. These results are enough accuracy for the fishery investigation.

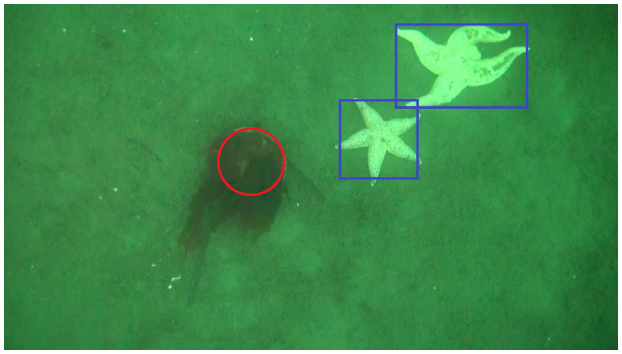

Figure 6. Experiment result sample. The object image is Fig. 2.

Table 2. Experiment results of the asteroid.

Detection Num.(tp)	293
Non-Detection Num.(tn)	1
Error Detection Num.(fn)	2
Detection Rate	99.66%
Error Rate	0.68%

4.3 Application of Analyzed Data

We made the resource maps of of the scallop and the asteroid with GPS data and the result data of Sect. 4.2. The GPS data was recorded at 10–20 seconds interval. Therefore, the location information's are used the linearly interpolated GPS data to correspond the seabed video.

The resource maps of the scallop and the asteroid are shown in Fig. 7. We can know the location information and the fishery resource information.

4.4 Discussion

In Sect. 4.2, the detection accuracy of the scallops are not enough because the algorithm to detect the scallop is the low accuracy in the ballas field. If this algorithm will apply this problem, the accuracy of the scallops is higher.

The detection accuracy of the asteroids are enough for the fishery investigation. However, there are the other asteroids such as *Luidia yesoensis*.

The fishery resource maps are very important for the fishery investigation. If these problems will be solved and the seabed videos are taken more, we can expect to increase the accuracy of the fishery resource maps (Fig. 7).

5 Conclusion

This paper has presented a method to detect the scallop and the asteroid from the seabed videos. In few visual features, this method defined the features of the scallop and the asteroid and models them on the basis of professional knowledge. Additionally, the experimental results gained by applying the proposed method to the seabed videos show our method to be useful. We applied the fishery resource map of the scallop and the asteroid using GPS data for the scallop culture industry.

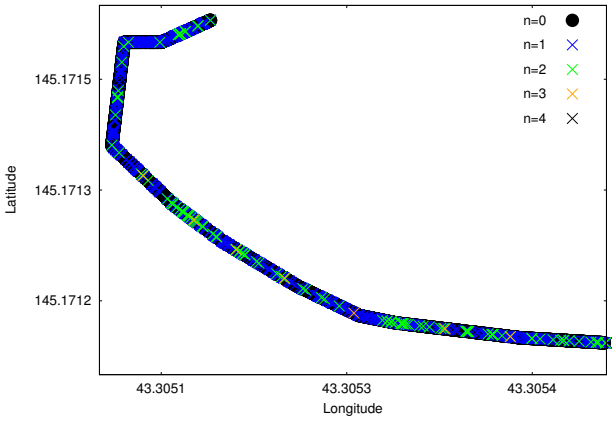

(a)

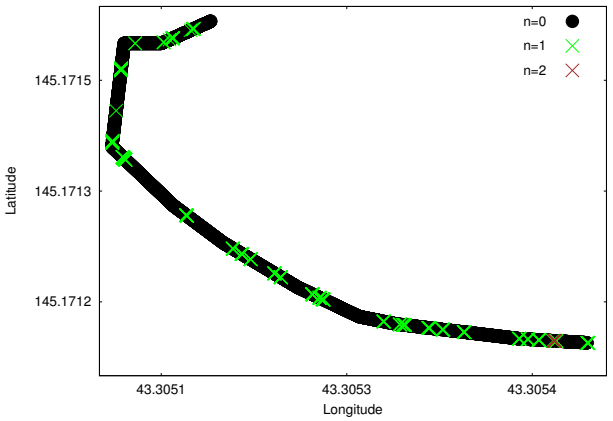

(b)

Figure 7. The fishery resource maps using the result data and the GPS data. The scallop resource map is (a) and the asteroid resource map is (b).

Future work, we will consider to introduce this system and develop the application due to the user can easily use.

References

[1] Hokkaido Abashiri Fisheries Experiment Station, "Monitoring Manual," Hokkaido Abashiri Fisheries Experiment Station, 2006.

[2] N. Honda and T. Watanabe, "Vertical distribution survey of the giant jellyfish Nemopilema nomurai by an underwater video camera attached to a midwater trawl net," *Bulletin of the Japanese Society of Scientific Fisheries*, vol. 73, no. 6, pp. 1042–1048, Nov. 2007.

[3] K. Enomoto, M. Toda, and Y. Kuwahara, "Extraction Method of Scallop Area in Gravel Seabed Images for Fishery Investigation," *Trans. IEICE*, vol. E93-D, no. 7, pp. 1754–1760, Jul. 2010.

[4] K. Enomoto, M. Toda, and Y. Kuwahara: "Extraction Method of Scallop Areas Using Shelly Rim Features Considering Bottom Sediment of Sand," Proc. of 8th IAPR Conference on Machine Vision Applications(MVA2011), pp. 263–266, Jan. 2011.